


ORIGINAL RESEARCH

Remediation and Treatment

Cobalt chromite nanoparticle effects on kapok diesel emulsion performance and emission characteristics at various injection pressures

B. Anbarasan¹  | K. Muralidharan¹ | C. Sakthi Rajan² | T. Rajkumar³

¹Department of Mechanical Engineering, PSNA College of Engineering and Technology, Dindigul, Tamil Nadu, India

²Department of Mechanical Engineering, SBM College of Engineering & Technology, Dindigul, Tamil Nadu, India

³Department of Mechanical Engineering, K. Ramakrishnan College of Technology, Trichy, Tamilnadu, India

Correspondence

B. Anbarasan, Department of Mechanical Engineering, PSNA College of Engineering and Technology, Dindigul 624 622, Tamil Nadu, India.

Email: anbarasan@psnacet.edu.in, anbarasan5mech@gmail.com

Abstract

Alternative fuels derived from vegetable oil have great potential as diesel fuel replacements in the transportation and manufacturing sectors. The aim of this study is to use cobalt chromite nanoparticles as a fuel additive with biodiesel in engine and to experimentally investigate the influence of injection pressure on combustion parameters. As an addition, cobalt chromite nanoparticles are used with biodiesel made from kapok oil, which is blended with mineral diesel at a ratio of 20:80. The engine is operated at various injection pressures (200–260 bar) and with an 80 ppm nanoparticle concentration. The results have shown that the increased injection pressure caused by the use of nanoparticles enhances engine combustion properties, such as the peak pressure and the rate of heat release. The main purpose of this research was to investigate the effects of a CoCr_2O_4 + KME20 mix on a CI engine, with the hope of improving engine performance characteristics. This investigation examines the effects of varying test fuel injection pressures. The increased injection pressure of CoCr_2O_4 + KME20 resulted in better performance and combustion. The 240-bar IP was shown to be superior to lower IPs because of its greater penetration length and more uniform formation. The IP rating of 240 bar represented a significant improvement over competing products with respect to emission controls. In addition to reducing our reliance on fossil fuels, this also prevents harmful chemicals from being released into the air.

KEYWORDS

biodiesel, cobalt chromite, engine, injection pressure, kapok methyl ester

1 | INTRODUCTION

The demand for energy is steadily rising on a daily basis, rendering it a vital component without which existence would be somewhat challenging in modern times. Currently, the predominant source of energy

is derived from fossil fuels. Since the 20th century, a number of researchers have concentrated on finding a possible substitute feedstock for diesel internal combustion (IC) engines owing to decreasing fossil fuel sources and strict pollution norms. If fossil fuel is utilized at the same rate as it is today, many studies have studied the making of methyl ester from different edible sources, for example neem oil, castor oil, soybean oil, sunflower oil, vegetable oils, and cotton seed oil. However, it is interesting to note that significant research efforts have also been dedicated to exploring non-edible sources of biodiesel.

Abbreviations: BSEC, brake specific energy consumption; BTE, brake thermal efficiency; CO, carbon monoxide; CoCr_2O_4 , cobalt chromite; D100, diesel; IP, injection pressure; KME 20, 80 diesel + 20 Kapok biodiesel; NO_x, oxides of nitrogen; UBHC, unburn hydrocarbon; UHC, unburn hydrocarbon.

These sources include jatropha, palm oil, animal fat, waste cooking oil, and canola etc.¹ Biofuel, specifically biodiesel, has emerged as a very efficacious option to supplant conventional diesel fuel. Biodiesel, or biofuel, can be readily utilized in modern diesel engines without requiring any retrofitting, enabling its direct use in IC engines. For the manufacture of biodiesel, organizations at the national and domestic levels currently exist. Biodiesel exhibits compatibility with existing fuel sources over a range of ratios, and possesses the capacity to function as a pure fuel in IC engines without the need for further additives. In India, the production of plant-based biofuel involves the utilization of several sources such as Pongamia, Jatropha, and mahua, among others. However, biodiesel has not yet been commercialized in India. The transport sector will undoubtedly become even more of a source of CO₂ emissions as the world's population and living standards rise. The worst consequences of climate change can be avoided if CO₂ emissions are reduced. Therefore, the automotive industry must adjust to new challenges; advancements like enhanced IC engines, electrifying the drive train, and replacing fossil fuels can help vehicles comply with emission regulations for greenhouse gases while simultaneously decreasing pollution.² The authors initiated the research, which involves the consumption of fuel mixtures consisting of rubber seed biodiesel and neat D100, with varying proportions of 20%, 40%, 60%, and 80% biodiesel. The injection pressure is set at 160 bar, while the compression ratio remains constant at 20. The tests are undertaken under varied supercharging instances, that is at 80% load. The experimental outcomes are compared with those of diesel, validating the substantial enhancements in performance and emission attributes achieved through the implementation of supercharging. The combustion properties of biodiesel blends are comparable to those of conventional diesel fuel.³ The researchers conducted the experiments varying the compression ratio (CR), and at CR18, both diesel fuel and 20Orange methyl ester (OME) showed similar trends in terms of HC and CO Pollutions. However, at CR 17, diesel fuel showed lower CO and HC emissions compared to 20OME. At lower loads, the fuel known as 20OME showed lower levels of NO_x emissions compared to diesel fuel when the CR was set at 17. However, when the CR was increased to 18, both fuels exhibited higher levels of NO_x emissions across all loads. A decrease in smoke emission was seen when using 20% oxygenated methyl ester (20OME) fuel compared to diesel fuel at both compression ratios.⁴ The studies were conducted by altering the compression ratio and using different proportions of waste oil methyl ester as biodiesel. Carbon monoxide, hydrocarbon, and carbon dioxide emissions are decreased as a result of the WOM40 blend, but nitrogen oxide emissions are increased. The research has determined that the combustion properties of waste cooking oil methyl ester and its diesel blends exhibit similar characteristics to those of conventional diesel.⁵ According to the experimental investigation, the engine for the B25 has a 4% higher thermal efficiency than traditional diesel. Also, the emissions and combustion results of a smaller amount of KME (B25) were the same as those of diesel fuel, which shows that KME could be used as an alternative fuel for diesel engines.⁶ The findings of the study indicate that the inclusion of ferric chloride as a fuel additive in waste cooking palm oil-based biodiesel led to a reduction in brake specific fuel consumption by 8.6%. Additionally, the BTE

experienced a notable rise of 6.3%. The inclusion of biodiesel via FBC resulted in decreased emissions of nitric oxide and a tiny increase in carbon dioxide emissions as compared to conventional diesel. At the optimum working condition of 280 bar injection pressure, the inclusion of FBC in biodiesel resulted in a reduction of CO emissions by 52.6%, total hydrocarbon (THC) emissions by 26.6%, and smoke emissions by 6.9% compared to biodiesel without FBC.⁷ Experimentally investigated the RSM-based predictive analysis of engine parameters of a CI engine fuelled with blend of D100/Aegle marmelos oil/(C₂H₅)₂O combinations at fluctuating CR, pressure, and timing of the injector. The experiment tests were conducted to portray the combined effects of CR, pressure, and timing of the injector on the engine analysis using all the test fuel with RSM (Response Surface Methodology). The result showed that increasing BTE and reduced carbon-based and nitrogen-based emissions.⁸ Experimentally investigated the advancement of timing in injecting the fuel and antioxidants for numerous responses of a CI engine fuelled with a blend based on algae and diesel. The authors tested conventional stationary engines with specified matrices and finally found the lesser impact of pyrogallol once equated with other influences for the NO_x emission control of the engine fuelled with a mixture of algae biodiesel.⁹ The authors performed combustion and emissions studies on a mixture of 30% waste palm oil (WPO). At an IP of 240 bar and an injection timing of 25.5° bTDC, the highest BTE of 31.3% was achieved. In comparison to diesel fuel, diestrol fuel exhibited a decrease in CO, CO₂, and smoke emissions by 33%, 6.3%, and 27.3%, correspondingly. The utilization of diestrol fuel resulted in a reduction of NO emissions by 4.3%. However, a slight raise in the levels of UBHC was recorded.¹⁰ Titanium dioxide oxide nanoparticles with concentrations of 50 ppm, 100 ppm, and 150 ppm were subjected to doping. Performance, emission, and combustion phenomena of a single-cylinder diesel engine were examined using Nano-blended waste plastic oil at three different fuel injection pressures, 210, 230, and 250 bar, respectively. According to the study, an acceptable substitute for diesel engines running at 230 bar of IP would be a blend of 150 ppm titanium dioxide and waste plastic oil.¹¹ The authors used the Optimal CR18 of injection pressure adjustment 170–290 bar with a interval of 20 bar, primary IP 210 bar to study the effect of IP on performance and emissions. The IP250 bar stands out as superior compared to other IP bars, resulting in a significant increase in BTE (32.51% at 100% load for NME40). When the engine is operating at maximum capacity and an intake pressure of 250 bar, the emissions of CO and HC are measured to be 1.79 and 0.016 g/kWh, correspondingly. The most commonly observed peak cylinder pressure is associated with an average pressure (IP) of 250 bar.¹² The authors adjusted the IP from 400 bar to 500 bar at 10 and 20 Nm loads at 1800 rpm. The ternary blends were put to the test in a CI engine. The outcomes revealed that DBOHep20 attained a extreme decrease in CO and smoke pollutions of 57.4% and 91.6%, correspondingly. The DBHep40 fuel had the lowest level of NO_x emissions, demonstrating a reduction of 13.27% compared to conventional diesel fuel.¹³ Researchers used diesel fuel at an IP of 220 bar as the baseline reading when analyzing the engine's performance and emission findings. The findings indicate that the brake thermal efficiency of the engine utilizing biodiesel exhibited a significant increase

of 8.94% and 16.09% respectively, when the fuel injection pressure was elevated from 220 bar - 240 bar at the rated power condition. Due to improved combustion, CO, HC, and smoke emissions were dramatically decreased by 22.32%, 14.23%, and 29.03%, respectively, at the IP of 260 bar.¹⁴ The authors of the studies combined biodiesel made from *Eichhornia Crassipes* with Nano sized titanium dioxide particles. CI engine is used to test three different biodiesel blends with titanium dioxide contents of 50, 100, and 150 ppm. The 150 ppm titanium dioxide blend is tested at a fuel injection pressure of 220 bar. The use of nanoparticles at high fuel IP increases BTE and reduces emissions. A comparative analysis reveals that the utilization of a Nano-blend biodiesel composition containing 150 ppm of titanium dioxide, when combined with a fuel IP of 220 bar, under maximum loading conditions, results in a considerable enhancement in BTE, with a maximum improvement of 1.01% when compared to the diesel mode.¹⁵ In recent years, there has been significant progress in the field of IC engine research, particularly in the development of techniques aimed at producing exceptionally low emissions and higher efficiency. This development has been driven by advancements in fuel injection and air charging technology. Considerable attention has also been directed towards carbon-free fuels.^{15–17} In this study, nanoparticles at the parts per million (ppm) level were used so that there was minimal environmental impact. The collection of nanoparticles from exhaust emissions was achieved through the utilization of a nanoparticle collecting method. Therefore, the release of nanoparticles into the environment has been significantly reduced. This helps to keep the environment clean and reduces the consumption of nanoparticles.¹⁶ According to the literature, researchers have primarily concentrated on different biodiesel blends with variable injection pressure, but very few studies have added nanoparticles with changes to engine parameters like injection pressure. The present research consequently proposes an investigation into the effects of kapok biodiesel and D100 mixture with the addition of different nanoparticles and varying the injection pressure in a conventional CI engine. In this study, the effects of mixing KME 20 with cobalt chromite nanoparticles and varying the injection pressures between 200 and 260 bar were examined. The objective of this present work is to determine the most optimal IP that results in higher combustion, improved performance, and lower emissions. The subsequent section will cover the methodology employed for the synthesis of biodiesel with nanoparticle materials.

2 | MATERIALS & METHODS

2.1 | Kapok seed oil

The scientific name of kapok is “*Ceiba pentandra*” and it is classified as a tree of the family Malvaceae. The size of the tree varied from 20 to 30 m in height and was found almost in all parts of South East Asia. An adult tree produces 500 woody seeds in a case formed one after another. Each and every case consists of 200–300 seeds that contain yellowish fiber. The fiber from the seed is made of cellulose which is up to 60% and they are widely used in pillows and mattresses manufacturing; kapok is the combination of cotton and seed, cotton is

used for pillow manufacturing; and seed is throughout like a waste, the seed is dark, which is common as it appears. Hence, the waste kapok seeds were collected from pillow manufacturing industries in Theni district. After that, kapok seeds were converted into raw oil. Kapok raw oil is a non-edible feedstock, was selected a superior source because of its ample availability and high raw oil yield, among other non-edible feedstocks. Figure 1 shows the kapok tree and seed.

The raw kapok oil extracted from the kapok seed is dark yellow and seems edible because of the pleasant smell, but it is non-edible because of the cyclopropenoid greasy acids in the oil. The presence of unsaturated fatty acids makes them preferable for utilization in engines. Table 1 shows the unsaturated fatty acids in Kapok oil methyl ester.

2.2 | Kapok oil extraction process

2.2.1 | Transesterification process

Transesterification is a process for segmenting the free fatty acid composition of methylester.¹⁵ Segmented fatty acids called methyl ester that belongs to the family of biodiesel blends, and the same is used in this research. For instance, if we separate the free fatty acid of kapok seed biodiesel, then it is called the methyl ester of kapok oil. The process is focused on reducing the viscosity of raw biodiesel extracted by the mechanical grinding method. The raw oil of kapok has high viscosity; hence, it cannot be directly used as fuel in the engine. So there is a need to reduce the viscosity of the raw kapok oil to an ASTM standard value because a high viscosity of fuel will lead to incomplete combustion due to poor atomization. To reduce the viscosity, there are many methods involved, some of which are as follows: preheating biodiesel before injection of the oil into the injector reduces the viscosity of the oil and another method is called transesterification and is explained in the upcoming sections. Transesterification is an equilibrium reaction involving various consecutive, reversible reactions. The method is used to remove the fatty acid alkyl esters from the triglycerides. Here, fatty acid alkyl esters are biofuel with reduced viscosity, and triglycerides are biodiesel with high viscosity. The process involves many process variables, such as temperature, nature of alcohol, molar ratio between oil and alcohol, catalyst type and influence of concentration of catalyst, purity of reactions, and intensity of mix. The process for intensifying the reaction is described using instruments such as microwaves, ultrasonic, supercritical fluids, and dynamic turbulence or co-solvents. The process of transesterification is as follows, as represented by Reference [16] (Figure 2).

The figure shows the reaction that takes place within the triglycerides and gives an output of fatty acid alkyl ester (Figure 3).

2.3 | Nano particles of cobalt chromite

Figure 5 displays a TEM image of cobalt chromite. Nanoparticles of cobalt chromite are included by a conventional co-precipitation method. Cobalt nitrate (0.5 M), chromium nitrate (1 M), and smelling

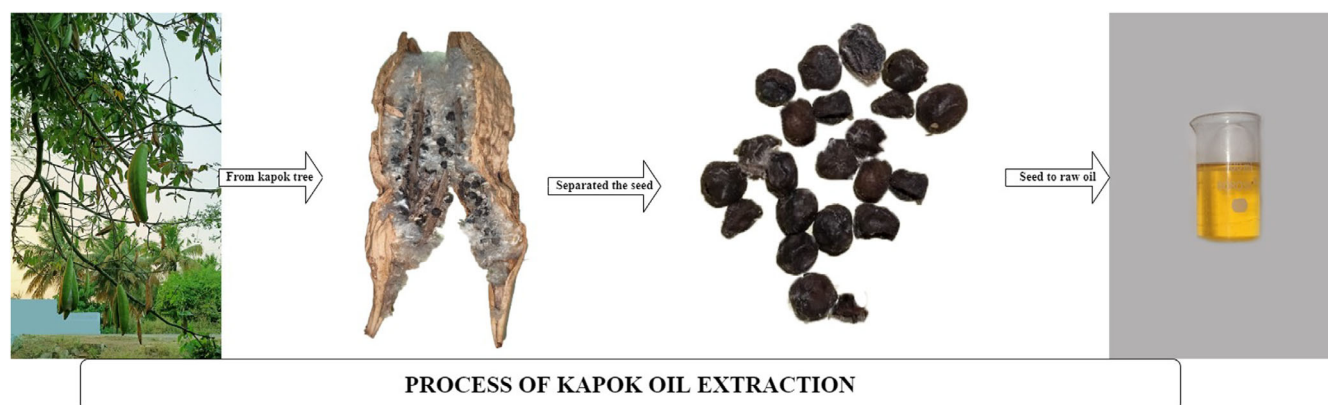


FIGURE 1 Steps involved in kapok oil extraction.

TABLE 1 Unsaturated fatty acids.

Name of the acid	Chemical formula	Percentages
Myristic acid	$C_{14}H_{28}O_2$	0.249%
Palmitic acid	$C_{16}H_{32}O_2$	24.30%
Palmitoleic acid	$C_{16}H_{30}O_2$	0.4%
Steric acid	$C_{55}H_{103}NO_{15}$	2.644%
Oleic acid	$C_{18}H_{34}O_2$	21.84%
Linoleic acid	$C_{18}H_{32}O_2$	38.92%
Arachidic acid	$C_{20}H_{40}O_2$	1.0%
Malvalic acid	$C_{18}H_{32}O_2$	7.2%
Sterculic acid	$C_{19}H_{34}O_2$	2.96%
Behenic acid	$C_{22}H_{44}O_2$	0.44%

salts (25%), were individually dissolved in an appropriate volume of distilled water and then arranged in 25 mL volumetric jars. The cobalt nitrate solution is measured out into a 100 mL glass, and the chromium nitrate solution is slowly added while stirring. The combined ingredients should be mixed together at room temperature for 2 h. The blended solution is adjusted to a pH of 9 by adding a smelling salt solution (with a concentration of 25%) drop by drop. We shift and wash the hydroxide accelerator numerous times. After relocating the hydroxide accelerator and rinsing it with clean water several times, the pH of the filtrate is predicted to be around 7.¹⁷ The resulting material is dried in a stove at 120°C for 16 h and then calcined at 600°C for 4 h, yielding a finely milled jasper green powder. Information on cobalt chromite can be found in Table 2. Figure 4 shows the UV spectra of cobalt chromite, and Figure 6 shows energy-dispersive X-ray spectroscopy (Figures 4–6).

2.4 | Test fuel preparation

Jasper green powder is obtained by leaving material to dry in a stove at 120°C for 16 h, followed by sintering at 600°C for 4 h, when the nanoparticles are formed and obtained. When it

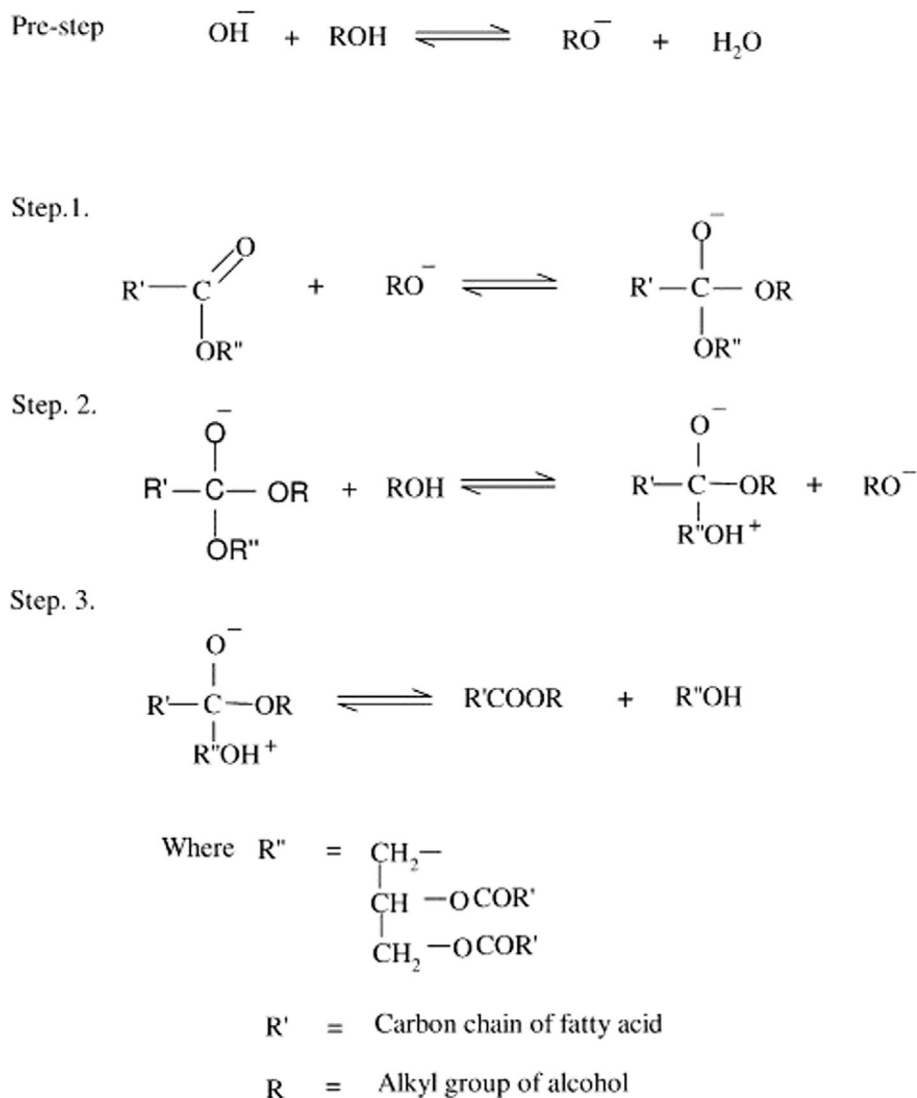
comes to oxygen concentration, cobalt chromite is the nanoparticle of choice. Blends are made by adding various amounts of kapok biodiesel to the main fuel source.¹⁸ The nanoparticles and the kapok biodiesel are mixed together by mechanical churning. The KME 20 blend is blended with various nanoparticle concentrations, including 20, 40, 60, and 80 ppm. This mixture has been produced and used as a test fuel, which is injected in the test engine at a pressure of 200–260 bar. The process of refining oil fuel is illustrated in Figure 3. The fuel's properties are enumerated in Table 3. Properties of the fuel are listed in Table 3.

2.5 | Uncertainty analysis

Error ranges are calculated by factoring in the degree of uncertainty present in the error analysis. The reading was influenced by the noise and heat from the gasoline engine. The diesel engine makes use of uncertainty analysis to cut down on many kinds of mistakes. Typically, a reading is collected after a diesel engine has been running for at least 30 min.¹⁹ Four or five separate readings are taken from the same blend, and the average of these values is used to create a graph. The degree of uncertainty is equal to the spread between the computed values and the experimental error. The outcomes of the uncertainty evaluation are displayed in Table 4.

2.6 | FTIR analysis

Figure 7, shows that kapok oil is represented by a peak that was obtained using FT-IR spectroscopy. Some very faint peaks at 1700–3000 cm^{-1} are present in kapok oil, and they seem to be in agreement with the CH band. In addition to cobalt chromite, biomolecules were also detected by FT-IR at 1236 cm^{-1} in the N-H band. After making the sample visible, the N–H band is seen because of the sharp peak at 3492 cm^{-1} , which is larger compared to the other generated peaks in this region, the aromatic ring and carbonyl

FIGURE 2 Step-by-step process of transesterification equation.

stretching modes. To get close to the NH_2 amine group, you can utilize a scissor-like in-plane twist at 1746 cm^{-1} .

2.7 | XRD analysis

Figure 8 depicts the results of an XRD investigation performed on kapok seed oil, revealing deflection peaks at 2, 46, and 66, which are linked to planes.¹⁹ Scherrer's technique estimates particle size distributions by measuring the peak of the deflection (1 1 1). Particles have an average size of 5.2 nm. In conclusion, the results show that kapok seed oil, on a similar nanoscale, is present in the sample and contributes to increased catalytic activity during the reaction.

3 | EXPERIMENTAL SETUP

Figure 9 shows the basic engine configuration for the study, which employs a typical single-cylinder, four-stroke, direct-ignition engine. Table 5 displays the basic engine's specifications. When the inspection

equipment is initially prepared for use, it is calibrated to the appropriate values for the exhaust emission parameters. The default setting for the engine speed is 1800 rpm, and the eddy current dynamometer is hooked up to the base engine to measure the output power of the engine. An AVL gas analyzer is used to measure various emission characteristics like CO, CO_2 , NO_x , and UBHC. The output power of the smoke meter is determined by employing an AVL 443 N apparatus. Table 6 shows the measuring range of the AVL gas analyzer. The readings were collected based on the experimental setup.

4 | RESULTS & DISCUSSION

4.1 | Combustion analysis

4.1.1 | In-cylinder pressure

The effect of various injection pressures of test fuel on In-Cylinder Pressure (ICP) generation is shown in Figure 10. The results of ICP rise with an increase in the IP of Nano blend biodiesel. It was evident that

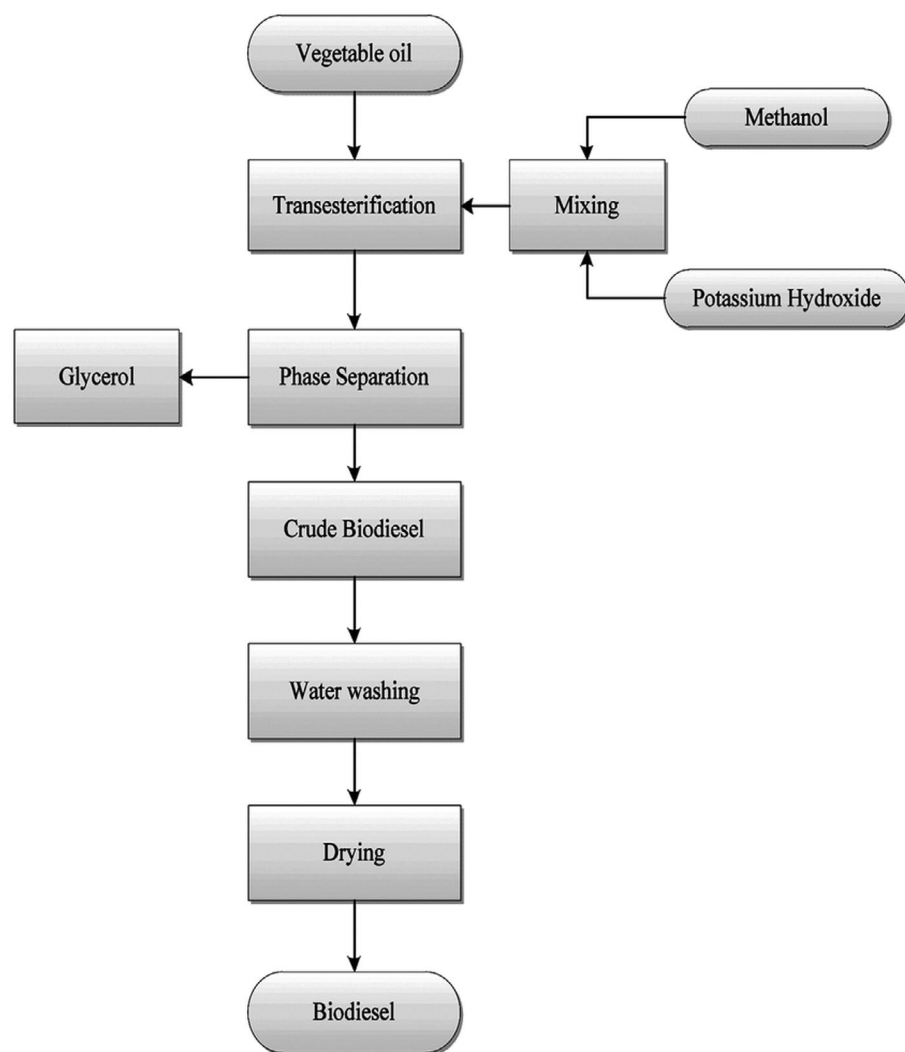


FIGURE 3 Process of biodiesel production.

TABLE 2 Free fatty acid composition of Kapok seed oil.

Fatty acid	Retention time (min)	g/100 g of fatty acid
Palmitic acid	5.89	22.37 ± 0.5
Stearic acid	8	3.8 ± 0.12
Malvalic acid	8.13	9.14 ± 0.1
Oleic acid	8.44	23.24 ± 0.41
Linoleic acid	9.23	33.63 ± 0.5
Sterculic acid	9.65	2.58 ± 0.15
Behenic acid	12.96	0.46 ± 0.05

Source: Anwar et al. (2014).

higher IP had a positive impact on the combustion process, which increased the ICP.¹⁹ This result would be due to a better A/F mixture and more air utilization because of fine fuel droplets.²⁰ From the result, it was noted that the ICP for IP of 200 bar was lower than diesel fuel at standard IP condition whereas higher IP of blends further improved the ICP reaching the peak level due to well atomization. The peak values of ICP for various IPs of CoCr_2O_4 + KME20 was 56.9, 61.4, 65.3 and 63.4 bar for 200, 220, 240 and 260 bar, respectively.

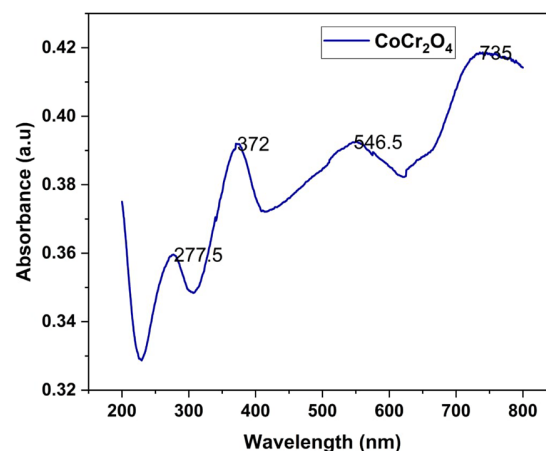


FIGURE 4 UV spectra of cobalt chromite.

The ICP value decreased by 4.39%, 11.40%, 16.73% and 14.21% for CoCr_2O_4 + KME20 at IPs of 200–260 bar with 20 bar interval, as compared to the KME20 blend at standard operating conditions. Moreover, the engine operated with CoCr_2O_4 + KME20 at IP of 220, 240 and

260 bar was noted to be 2.5%, 8.4% and 5.6% higher than diesel fuel under normal conditions. This result indicated that higher injection pressure, fine atomization, shortened ID, and better combustion efficiency, therefore, generate higher post-combustion pressure.²¹

4.1.2 | Heat release rate

Figure 11 exhibits the difference in HRR for test fuel with various injection pressures at CR 19. The results of HRR improved with the rise in IP of the nanoparticle-enriched KME20 blend. Generally, an increase in

the HRR was directly proportional to an increase in the cylinder pressure. From the results, it was proved that the high peak cylinder pressure of IP 240 bar showed maximum HRR. This reasonable increment was caused by improved combustion quality and a higher oxidation rate of fuel. The figure exhibited that the IP of 240 bar displayed a maximum HRR of 83.1 J/°CA, followed by the IP of 260 bar which was 77.3 J/°CA, IP of 220 bar it was 71.8 J/°CA and diesel at standard IP, it was 69.6 J/°CA. The peak value of HRR decreased by 2.4% for the CoCr₂O₄ + KME20 blend at 220 bar, 16.4% for the CoCr₂O₄ + KME20 blend at 240 bar, and 10.7% for the CoCr₂O₄ + KME20 blend at 260 bar when compared to diesel fuel at 220 bar for peak load condition. The higher level of HRR was noticed because of the increased pressure in the injector nozzle with high CR, resulting in a better peak cycle temperature.^{19,22} This result might be due to the benefits of elevated IP and the more turbulent motion of the mixture. It leads to a shortening of the delay period, and thereby, results in high combustion fraction in primary phase of combustion.

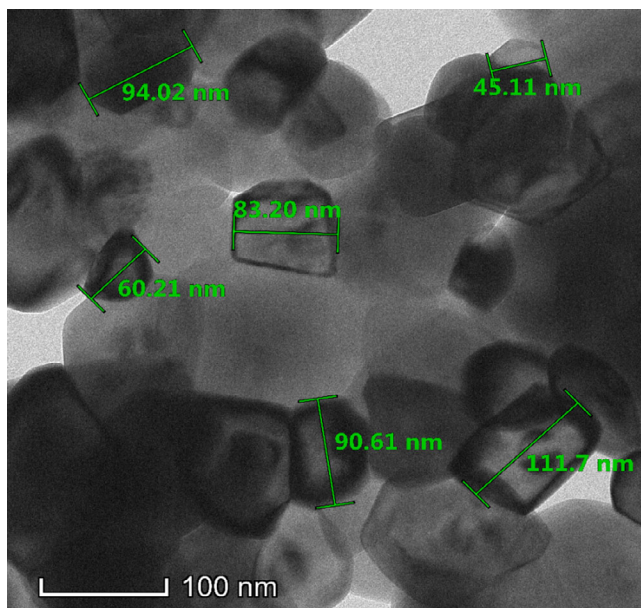


FIGURE 5 TEM images of cobalt chromite nano-particles.

TABLE 3 Fuel properties.

Property	Diesel	Raw oil	KME20 + 80 ppm
Specific gravity (40°C) (kg/m ³)	0.85	0.875	0.846
Density (40°C) (kg/m ³)	822	931	864
Viscosity (40°C) (mm ² /S)	3.1	4.2	3.1
Calorific value (MJ/m ³)	44	38	39
Cetane number	54	48	53
Acid number	-	0.2	0.1
Fire point (°C)	74	174	158
Flash point (°C)	59	170	162

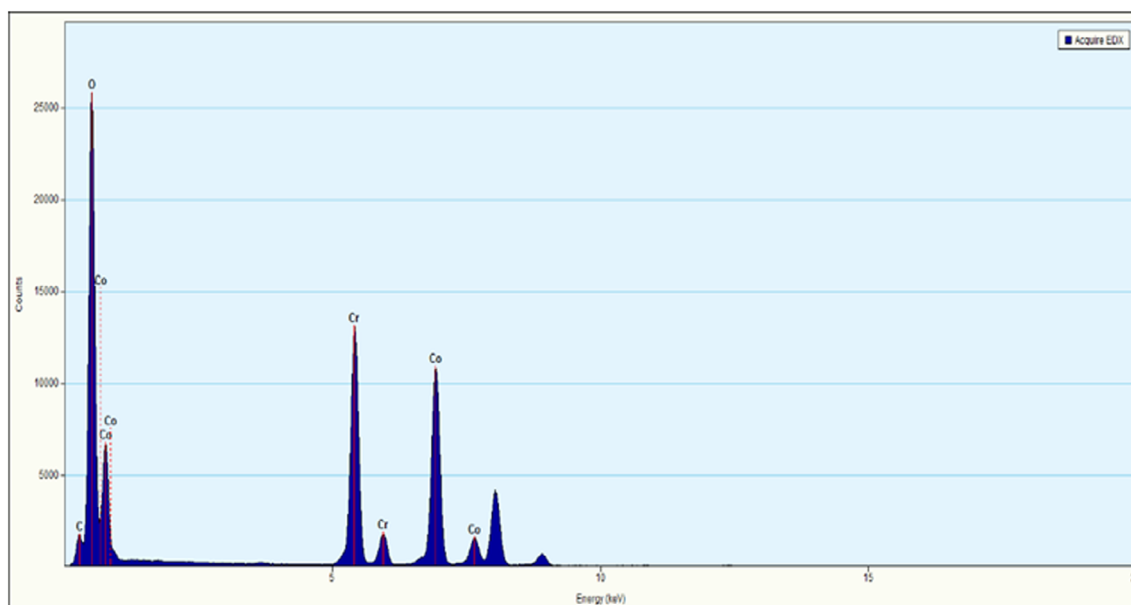


FIGURE 6 Energy-dispersive X-ray spectroscopy EDX).

4.2 | Performance analysis

4.2.1 | BTE

Figure 12 evaluates the thermal efficiency with BP for fuel Kapok methyl ester and its blends at different injection pressures (IP). The improved thermal efficiency was observed for KME20 with nanoparticles at higher injection pressure. The thermal efficiency at peak load was improved by 1.74% for $\text{CoCr}_2\text{O}_4 + \text{KME20}$ blend at 220 bar, 5.83% for $\text{CoCr}_2\text{O}_4 + \text{KME20}$ at 240 bar and 3.9% for $\text{CoCr}_2\text{O}_4 + \text{KME20}$ blend at 260 bar when associated with diesel fuel at 220 bar. It can be attributed to the improved vaporization characteristics of biodiesel while increasing the injection pressure²³ This results in a quick burn and releases more heat energy, improving combustion efficiency¹⁹ As a result, the exhaust temperature of biodiesel and its blends was higher than diesel. For higher IP, the maximum BTE was achieved at all load conditions. This was because the fine fuel

droplet completely diffuses with the air in the cylinder, which enhances the combustion rate. From the results, lower thermal efficiency was observed at the initial load condition for all test fuels. In contrast, peak load conditions showed superior performance due to an increase in the cylinder temperature, therefore improving fuel vaporization. It was evident that the BTE of $\text{CoCr}_2\text{O}_4 + \text{KME20}$ at 240 bar was 4.1% and 7.3% higher than other IPs. The results exhibited a marked increase in fuel penetration length and the breaking down of the fuel particles, which enhanced the homogeneous formation. The result of BTE was 29.23%, 30.2%, 31.5% and 30.9% for the blend of $\text{CoCr}_2\text{O}_4 + \text{KME20}$ at IP of 200, 220, 240 and 260 bar, respectively. These results also showed that an increase in the IP beyond 240 bar had a negative effect on thermal efficiency because fuel particles impinged on the chamber wall and skipped the combustion process.²⁴

4.2.2 | Brake specific energy consumption

The difference in brake-specific energy consumption for various test fuels at peak load conditions is shown in Figure 13. The results exhibit that the energy consumption of the fuel was higher for lower load conditions and gradually reduced with the rise of the load. The marginal reduction in energy consumption at a higher load improves the combustion rate. At peak load, IP of 240 bar showed a sharp reduction in BSEC with Nano blend KME20. For standard IP, the result of BSEC was 12.12 MJ/kWh and 13.17 MJ/kWh for diesel and KME20 without nano additive. It was noticed that the energy consumption was higher for KME20 as compared to the same fuel doped with the nanoparticle. The BSEC for the $\text{CoCr}_2\text{O}_4 + \text{KME20}$ blend at various IPs of 200, 220, 240 and 260 bar was 12.31, 11.91, 11.41 and 11.64 MJ/kWh, respectively. It was mainly due to an increase in the injection pressure, which leads to the atomization of fuel that results in complete combustion. In

TABLE 4 Uncertainty analysis.

S. no.	Parameters	Systematic errors
1	Speed (rpm)	± 1.00
2	Load (N)	± 0.20
3	Time (sec)	± 0.10
4	Brake power (kW)	± 0.50
5	Temperature ($^{\circ}\text{C}$)	± 1.00
6	Pressure (bar)	± 1.00
7	NO_x (ppm)	± 9.00
8	CO (%)	± 0.03
9	CO_2 (%)	± 0.03
10	UBHC (ppm)	± 10.00
11	Smoke (HSU)	± 1.00

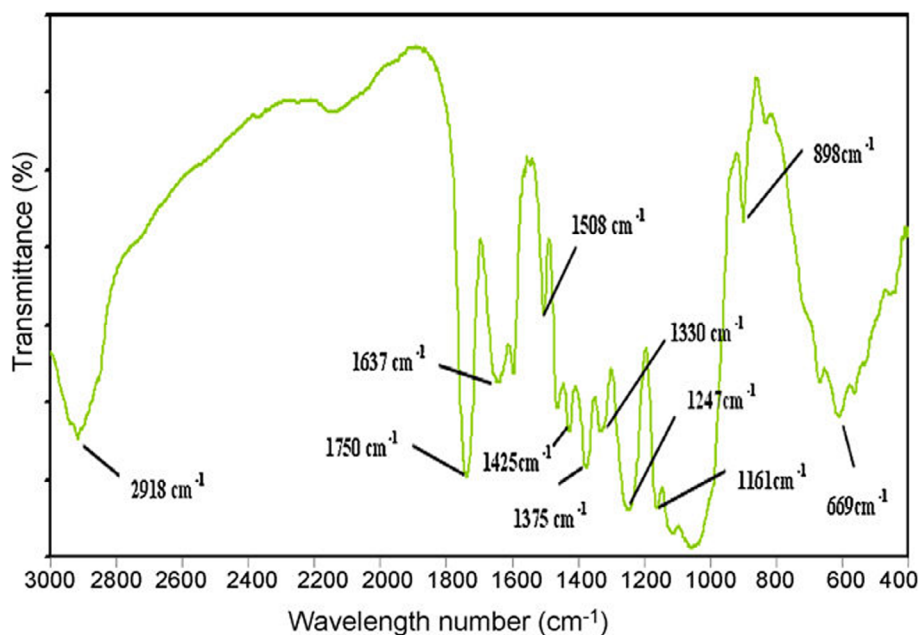


FIGURE 7 FTIR analysis for kapok oil.

FIGURE 8 XRD analysis for kapok oil.

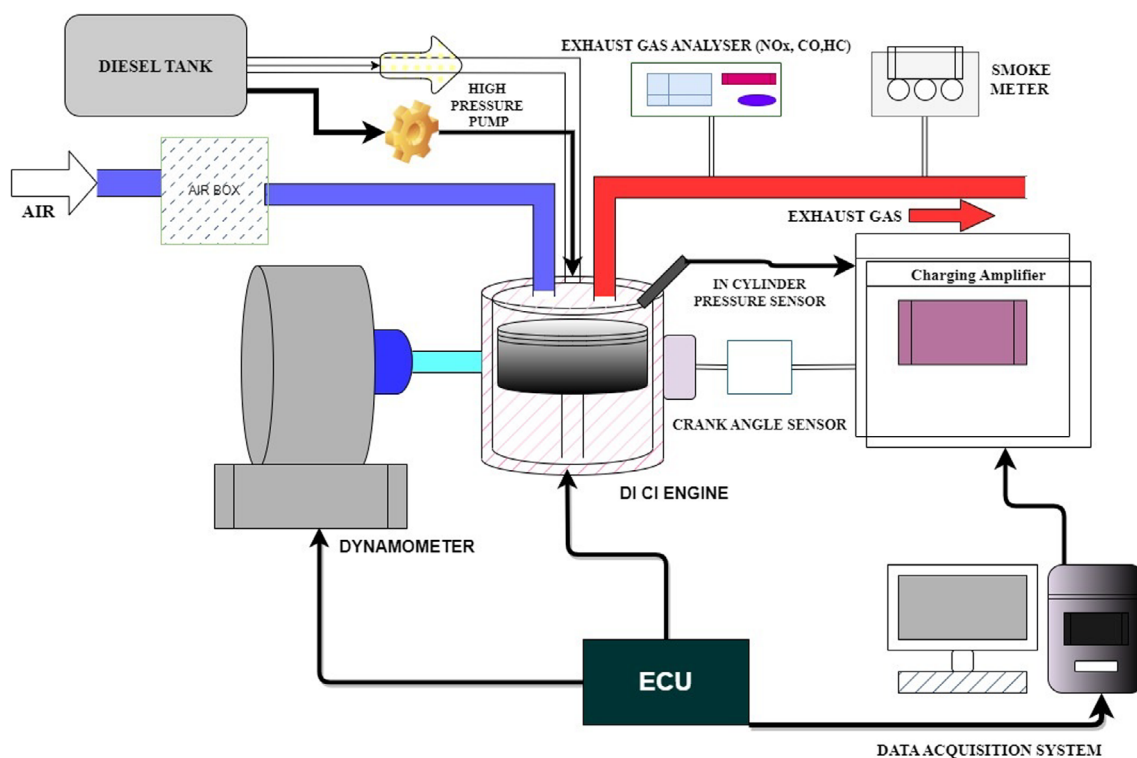
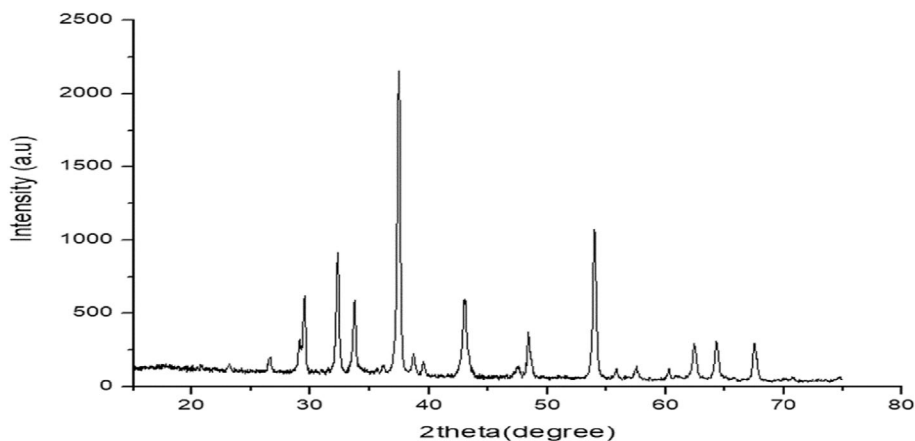


FIGURE 9 Experimental setup.

addition, the energy consumption was reduced by 2.2% for the $\text{CoCr}_2\text{O}_4 + \text{KME20}$ blend at 220 bar, 5.6% for $\text{CoCr}_2\text{O}_4 + \text{KME20}$ at 240 bar and 4.5% for the $\text{CoCr}_2\text{O}_4 + \text{KME20}$ mixture at 260 bar when compared to D100 fuel at 220 bar for peak load conditions. This result could be attributed to the positive impact of shorter ID and improved homogenous formation, whereas IP beyond 260 bar slightly increases the BSEC. It can be ascribed to wall impingement and heterogeneous mixture formation that result in incomplete combustion. $\text{CoCr}_2\text{O}_4 + \text{KME20}$ injected at the rates of 240 and 260 bar was 4.2% and 2.9% lower, respectively, as compared to the same blend at standard IP. This could be ascribed to improved fuel vaporization and elevated fuel penetration, which gives a better combustion rate.²⁵

4.3 | Emission analysis

4.3.1 | Carbon monoxide

Figure 14 depicts the assessment of CO emissions in the $\text{CoCr}_2\text{O}_4 + \text{KME20}$ blend at various injection pressures (IPs). The findings indicate a notable reduction in CO emissions as the engine load increases. The lowest CO emission occurred at an IP of 240 bar. Additionally, CO emissions were lower under initial load conditions, escalating to peak values at high load conditions, possibly attributable to a rich fuel zone and low cylinder temperature.^{25–27}

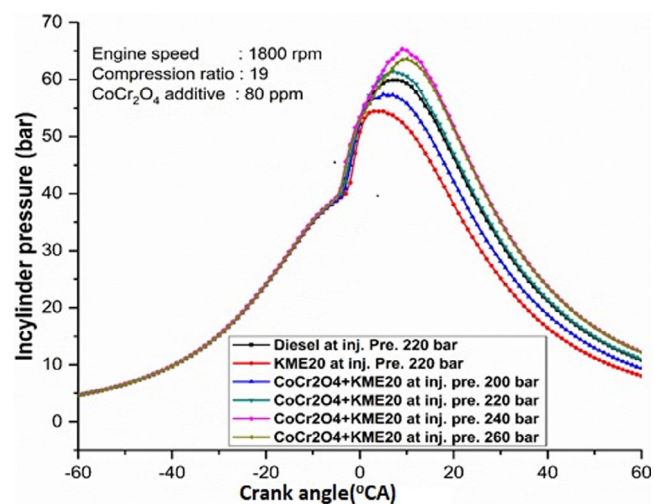
The CO emission results for $\text{CoCr}_2\text{O}_4 + \text{KME20}$ at different IPs 200–260 bar were 4.05, 3.69, 3.26, and 3.41 g/kWh, respectively.

TABLE 5 Specification of engine.

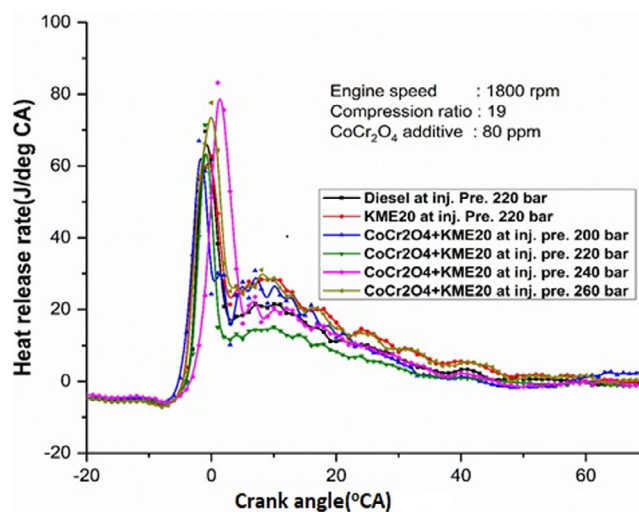
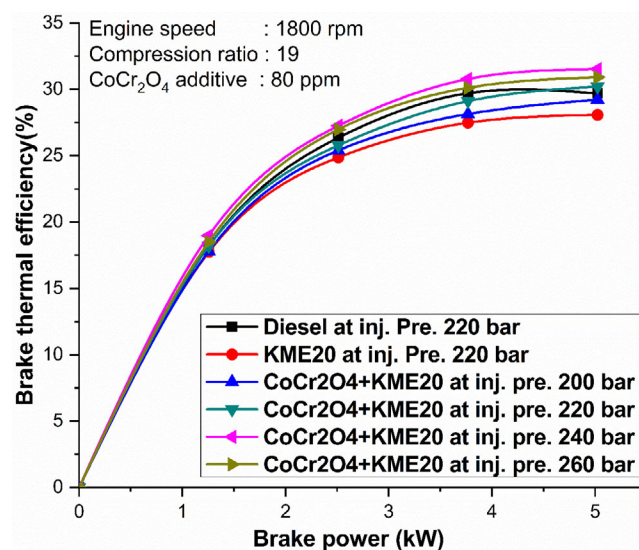
Specification of engine	
Brand, model	Kirloskar, SV1
Number of cylinder	1
Cooling type	Water-cooled
Stroke volume	661 cc
Engine speed	1800 rpm (constant)
No. of strokes	4
Clearance volume	37.8 cc
Rated output	5.9 kW
Diameter of bore	87.5 mm
Length of stroke	110 mm
Lubrication system	Forced feed system
Compression ratio	19:1

TABLE 6 Measuring range of AVL Gas analyzer.

Sl. no	Exhaust gas	Measuring range
1	UBHC	0–20,000 ppm Vol
2	CO	0%–10% vol.
3	NO _x	0–5000 ppm
4	O ₂	0%–22 vol.%
5	CO ₂	0%–20% vol

**FIGURE 10** Variation of In-cylinder pressure with crank angle for different IP at CoCr₂O₄ + KME20 blend.

Notably, higher injection pressure led to a significant reduction in CO emissions, attributed to enhanced post-combustion temperature and oxidation rate. Specifically, CO emissions were reduced by 13.01% at 200 bar, 20.01% at 220 bar, 29.76% at 240 bar, and 26.5% at 260 bar for the CoCr₂O₄ + KME20 blend than diesel fuel at 220 bar under high load conditions. This reduction can be

**FIGURE 11** Variation of HRR with crank angle for different IP at CoCr₂O₄ + KME20 blend.**FIGURE 12** Variation of BTE with brake power for various IP.

ascribed to the high injection pressure promoting a favorable air/fuel (A/F) ratio, resulting in optimal combustion rates and lower CO formation.

Remarkably, CO emissions decreased with increasing IP up to 240 bar; however, beyond this point, a rapid increase occurred, attributed to quenching effects and the presence of a fuel-rich zone, limiting CO conversion.

4.3.2 | Unburnt hydrocarbon

Figure 15 illustrates the trend of UBHC (unburned hydrocarbon) emissions for the fuel CoCr₂O₄ + KME20 under various injection pressures. The findings reveal that diesel fuel exhibited higher UBHC

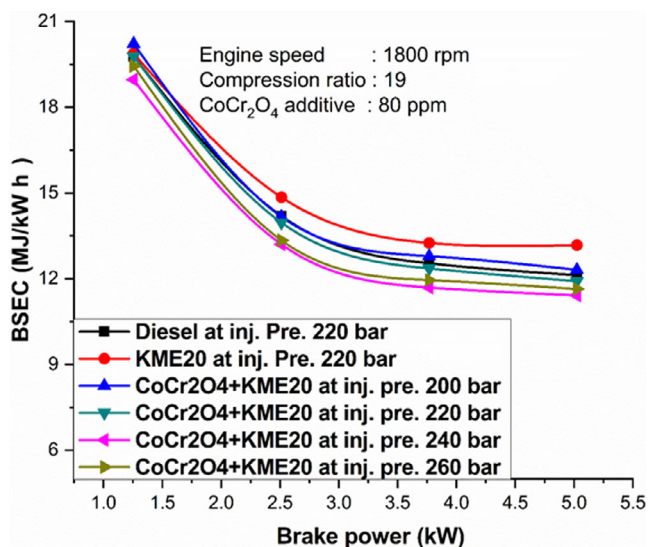


FIGURE 13 Variation of BSEC with brake power for various IP.

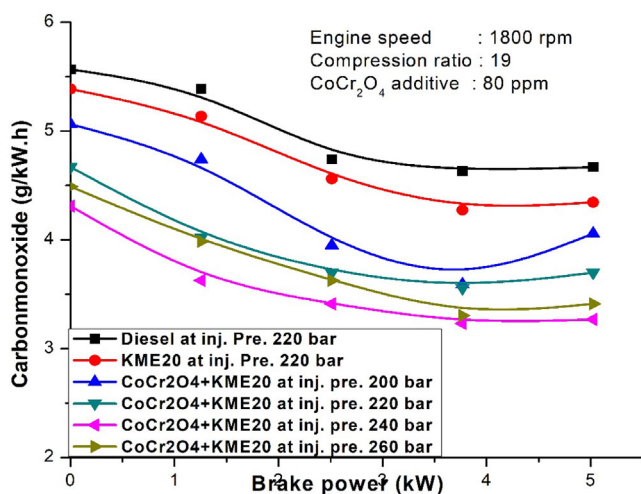


FIGURE 14 Variation of CO with brake power for various IP.

emissions compared to $\text{CoCr}_2\text{O}_4 + \text{KME20}$ across all injection pressure conditions. This discrepancy can be attributed to the inherent oxygen content and elevated exhaust gas temperature of biodiesel, facilitating partial combustion. Increased combustion rates resulted in a reduction of UBHC emissions.

At the standard injection pressure (IP), a blend of nanoparticles with KME20 showed a 6.9% decrease in UBHC emissions than a diesel blend. This reduction can be attributed to the positive impact of the catalytic activity of the nanoparticles and the abundant oxygen supply in the cylinder, leading to a more efficient combustion process. Furthermore, an elevation in the injection pressure gradually decreased UBHC emissions due to fuel vaporization, charge pressure, and temperature. The UBHC emission values for the nanoparticle blend were 0.088, 0.082, 0.098, and 0.106 g/kWh for injection pressures of 260, 240, 220, and 200 bar, respectively. This can be

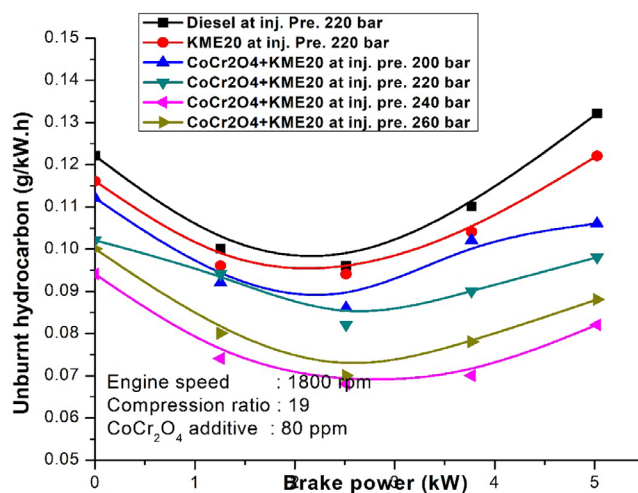


FIGURE 15 Variation of UBHC with brake power for various IP.

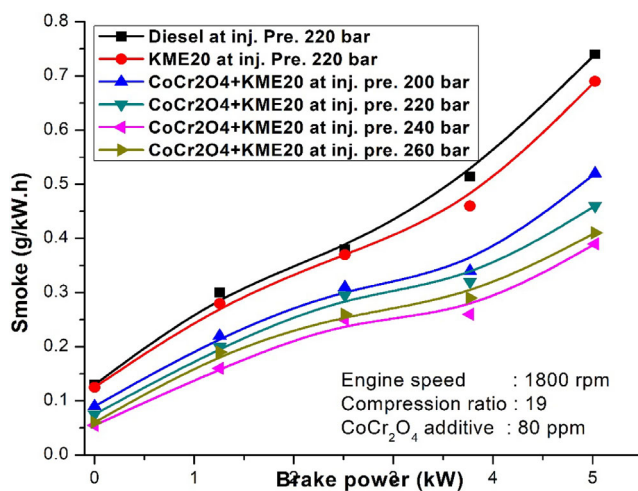


FIGURE 16 Variation of smoke with brake power for various IP.

attributed to enhanced air utilization and a longer penetration length of fuel, promoting increased partial combustion.

Comparatively, the UBHC emission of diesel at an IP of 220 bar exhibited increases of 19.6%, 25.7%, 37.8%, and 33.3% for $\text{CoCr}_2\text{O}_4 + \text{KME20}$ at 200, 220, 240, and 260 bar injection pressures, respectively, under full load conditions. This escalation was primarily influenced by a combination of factors, including higher oxygen levels, nano-catalytic activity, and the presence of fine fuel droplets, collectively contributing to an improved combustion rate.²⁸

4.3.3 | Smoke

Figure 16 illustrates the variations in smoke production among diesel, KME20, and a blend of the two with a nanoadditive at different injection pressures. In comparison to biodiesel blends and pure

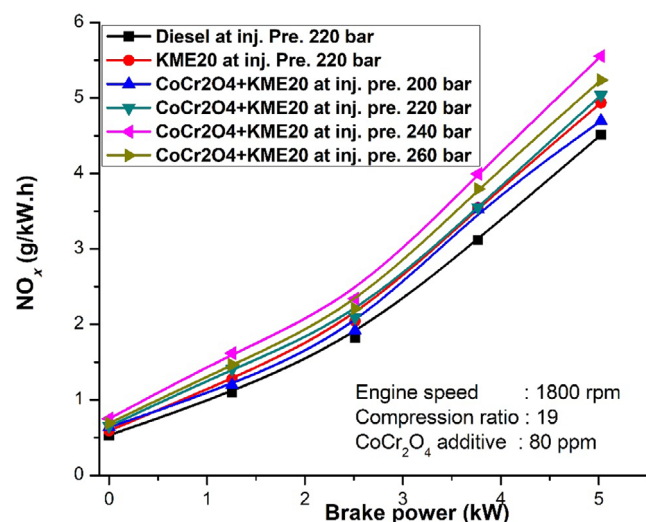


FIGURE 17 Variation of NO_x with Brake power for various IP.

biodiesel, the CI engine running on diesel fuel exhibited elevated levels of smoke. Additionally, it was observed that injecting the test fuel at standard pressure resulted in higher smoke emissions than at an increased IP. At peak load, the smoke emissions of CoCr₂O₄ + KME20 at different injection pressures were as follows: 0.52 g/kWh at 200 bar, 0.46 g/kWh at 220 bar, 0.39 g/kWh at 240 bar, and 0.41 g/kWh at 260 bar. Notably, injection pressure of 240 bar demonstrated the lowest smoke emission under peak load conditions. The rise in injection pressure correlated with a reduction in smoke emissions, attributed to improved fine atomization and a more complete burn rate. However, beyond 240 bar, a negative trend was observed due to increased penetration and wall wetting.^{28–30}

Furthermore, KME20 exhibited a significant decrease in smoke emissions when combined with nanoparticles, owing to the catalytic activity of the nanoparticles generating excess O₂ in the chamber. At an IP of 240 bar, the smoke emission was 25%, 11.3%, and 4.67% lower than at 200, 220, and 260 bar IPs, respectively, under rated BP conditions. This reduction was attributed to the formation of a suitable homogeneous fuel-air mixture with a high burning rate.

In contrast, the smoke emissions of diesel at an IP of 220 bar were 29.7%, 37.8%, 47.2%, and 44.5% higher than those of CoCr₂O₄ + KME20 at IPs of 200, 220, 240, and 260 bar, respectively, under full load conditions. This effect was attributed to the triple combination of inherent O₂ in biodiesel, enhanced chemical reactions, and improved fuel vaporization, resulting in superior fuel oxidation.³¹

4.3.4 | Nitrogen oxide

Figure 17 illustrates the assessment of NO_x emissions concerning diesel, KME20, and their Nano blends under different injection pressures (IPs). The NO_x emission levels rose proportionally with increasing injection pressure. As depicted in the figure, NO_x emissions linearly increased up to 50% of the load, reaching their peak at full load. This

escalation was primarily due to the greater quantity of burned fuel, leading to intensified heat release within a shorter time frame.

Notably, the incorporation of nanoparticles with KME20 at an IP of 240 bar resulted in NO_x emissions that were 18.5% and 11.3% higher than diesel and KME20 at the standard injection pressure. This rise in NO_x emissions was attributed to the secondary atomization of fuel resulting from nanoparticle doping, a phenomenon previously identified by Reference [32].

Analyzing the variation in injection pressure, it was observed that a higher pressure of approximately 240 bar led to the maximum NO_x emissions. This outcome was attributed to minimized combustion duration and an improved primary combustion zone, promoting homogeneous combustion and elevated cylinder temperatures. However, further increasing the IP beyond 240 bar showed a decreasing trend in NO_x emissions due to overmixing of the charge and a longer penetration length, leading to fuel impingement at the cylinder wall and consequently inferior combustion.³³

In the case of the CoCr₂O₄ + KME20 blend, NO_x emissions were reduced by 3.9% at 200 bar, 10.4% at 220 bar, 18.7% at 240 bar, and 13.8% at 260 bar compared to diesel fuel at 220 bar under peak load conditions. The data highlighted that an IP of 240 bar resulted in higher NO_x emissions than other test conditions, attributed to its positive impact on ignition delay and a shorter combustion duration, minimizing the diffusion combustion phase.

5 | CONCLUSION

Enhancing the engine performance parameters with a CoCr₂O₄ + KME20 blend on a CI engine was the prime aim of the current research. The superior performance and combustion were noticed as a result of the higher injection pressure of the CoCr₂O₄ + KME20 blend. Due to its higher penetration length and homogeneous formation, the IP of 240 bar was noticed to be better than other IPs. Also, an IP of 240 bar was a drastic reduction in emission parameters than its rivals. This could be attributed to better mixing of the A/F mixture and a quick fuel vaporization rate.

- The performance parameter of BTE was 7.3%, 4.2% and 1.9% lower for nanoparticle blend KME20 at IP of 200, 220 and 260 bar, correspondingly, as compared to IP of 240 bar for the same fuel.
- The specific energy consumption of CoCr₂O₄ + KME20 injected at a rate of 240 bar was 2.9% lower as related to the same blend at standard IP.
- The combustion pressure of CoCr₂O₄ + KME20 at an IP of 240 bar was 8.4% higher than diesel fuel under normal conditions at a standard IP.
- The peak value of HRR was increased by 16.4% for the CoCr₂O₄ + KME20 mixture at 240 bar than diesel fuel at 220 bar for peak load conditions.
- The CO emission was minimized by 29.76% for CoCr₂O₄ + KME20 at 240 bar than diesel fuel at 220 bar for maximum load conditions.

- The UBHC emission of diesel at an IP of 240 bar was 37.8% CoCr_2O_4 + KME20 at an IP of 240 bar at peak load conditions when compared to standard injection pressure.
- For CoCr_2O_4 + KME20 at an IP of 240 bar under maximum load conditions, the smoke emission decreased by 47.2%.
- The NO_x emission was increased by 18.7% for CoCr_2O_4 + KME20 at 240 bar when than diesel fuel at 220 bar for maximum load conditions at normal injection pressure.

From the above observation, it has been found that KME 20 with 80 ppm cobalt chromite nanoparticles and an IP of 240 bar gives better performance compared with other injection pressures at compression ratio 19. The emissions of CO and UBHC are lesser compared to diesel fuel, but the NO_x emissions are slightly increased than other injection pressures; it will be in the acceptable range compared with standard diesel fuel.

5.1 | Scope of future research

- The current investigation including the utilization of KME 20 with 80 ppm bio nanoparticles and engine alteration exhibits potential for future research extension.
- The implementation of an after treatment device such as a lean NO_x trap or Selective Catalytic Reduction, Exhaust Gas Recirculation is required to achieve a thorough drop in NO_x emissions.
- Further research was conducted with an advanced common rail direct injection system and HCCI Engine.

AUTHOR CONTRIBUTIONS

B. Anbarasan: Conceptualization; investigation; methodology; writing – original draft. **K. Muralidharan:** Supervision. **C. Sakthi Rajan:** Formal analysis. **T. Rajkumar:** Formal analysis.

CONFLICT OF INTEREST STATEMENT

The authors declare that they have no conflict of interest.

DATA AVAILABILITY STATEMENT

The data that support the findings of this study are available from the corresponding author upon reasonable request.

ORCID

B. Anbarasan  <https://orcid.org/0000-0002-7032-3417>

REFERENCES

1. Ramkumar S, Kirubakaran V. Biodiesel from vegetable oil as alternate fuel for CI engine and feasibility study of thermal cracking: a critical review. *Energy Convers Manage*. 2016;118:155-169.
2. Shukla PC, Belgiorno G, Di Blasio G, Agarwal AK. Introduction to alcohol as an alternative fuel for internal combustion engines. *Alcohol as an Alternative Fuel for Internal Combustion Engines*. Singapore; 2021:1-4.
3. Murugapoopathi S, Vasudevan D. Performance, combustion and emission characteristics on VCR multi-fuel engine running on methyl esters of rubber seed oil. *J Therm Anal Calorim*. 2019;138:1329-1343.
4. Karthickeyan V, Dhinesh B, Balamurugan P. Effect of compression ratio on combustion, performance and emission characteristics of DI diesel engine with orange oil methyl ester. *Bioresour Utiliz Bioprocess*. 2020;131-149.
5. Muralidharan K, Vasudevan D, Sheeba KN. Performance, emission and combustion characteristics of biodiesel fuelled variable compression ratio engine. *Energy*. 2011;36(8):5385-5393.
6. Vedharaj S, Vallinayagam R, Yang WM, Chou SK, Chua KJE, Lee PS. Experimental investigation of kapok (*Ceiba pentandra*) oil biodiesel as an alternate fuel for diesel engine. *Energy Convers Manage*. 2013;75:773-779.
7. Kannan GR, Karvembu R, Anand RJA. Effect of metal based additive on performance emission and combustion characteristics of diesel engine fuelled with biodiesel. *Appl Energy*. 2011;88(11):3694-3703.
8. Subramani S, Natarajan K, Rao GLN. Optimization of injection timing and anti-oxidants for multiple responses of CI engine fuelled with algae biodiesel blend. *Fuel*. 2021;287:119438.
9. Kannan GR, Anand R. Experimental evaluation of DI diesel engine operating with diestrol at varying injection pressure and injection timing. *Fuel Process Technol*. 2011;92(12):2252-2263.
10. Sundar SP, Vijayabalan P, Sathyamurthy R, Said Z, Thakur AK. Experimental and feasibility study on nano blended waste plastic oil based diesel engine at various injection pressure: a value addition for disposed plastic food containers. *Fuel Process Technol*. 2023;242:107627.
11. Dash SK, Lingfa P, Das PK, Saravanan A, Dash D, Bharaprasad B. Effect of injection pressure adjustment towards performance, emission and combustion analysis of optimal nahar methyl ester diesel blend powered agricultural diesel engine. *Energy*. 2023;263:125831.
12. Khan MM, Kadian AK, Sharma RP. Investigation of high fuel injection pressure variation on compression ignition engines powered by jatropha oil methyl ester-heptanol-diesel blends. *Alex Eng J*. 2023;65:675-688.
13. Selvaraj K, Thangavel M. The effects of fuel injection pressure on combustion and emission characteristics of a diesel engine using frying oil methyl ester. *Energy Sources A: Recov Utiliz Environ Eff*. 2023;45(3):7436-7452.
14. Jain A, Bora BJ, Kumar R, et al. Impact of titanium dioxide (TiO_2) nanoparticles addition in *Eichhornia crassipes* biodiesel used to fuel compression ignition engine at variable injection pressure. *Case Stud Therm Eng*. 2023;49:103295.
15. Di Blasio G, Ianniello R, Beatrice C, Pesce FC, Vassallo A, Belgiorno G. Additive manufacturing new piston design and injection strategies for highly efficient and ultra-low emissions combustion in view of 2030 targets. *Fuel*. 2023;346:128270.
16. Sahu TK, Shukla PC, Belgiorno G, Maurya RK. Alcohols as alternative fuels in compression ignition engines for sustainable transportation: a review. *Energy Sources A: Recov Utiliz Environ Eff*. 2022;44(4):8736-8759.
17. Belgiorno G, Di Blasio G, Beatrice C. Advances of the natural gas/diesel RCCI concept application for light-duty engines: comprehensive analysis of the influence of the design and calibration parameters on performance and emissions. *Nat Gas Engines: Transport Power Gener*. 2019;251-266.
18. Kumar S, Dinesha P, Bran I. Influence of nanoparticles on the performance and emission characteristics of a biodiesel fuelled engine: An experimental analysis. *Energy*. 2017;140:98-105.
19. Kanth S, Ananad T, Debbarma S, Das B. Effect of fuel opening injection pressure and injection timing of hydrogen enriched rice bran biodiesel fuelled in CI engine. *Int J Hydrogen Energy*. 2021;46(56):28789-28800.
20. Gong C, Si X, Liu F. Effects of injection timing and CO_2 dilution on combustion and emissions behaviors of a stoichiometric GDI engine under medium load conditions. *Fuel*. 2021;303:121262.
21. Hatami M, Hasanpour M, Jing D. Recent developments of nanoparticles additives to the consumables liquids in internal combustion engines: part II: Nano-lubricants. *J Mol Liq*. 2020;319:114156.

22. Jamshaid M, Masjuki HH, Kalam MA, Zulkifli NWM, Arslan A, Qureshi AA. Experimental investigation of performance, emissions and tribological characteristics of B20 blend from cottonseed and palm oil biodiesels. *Energy*. 2022;239:121894.
23. Ogunkunle O, Ahmed NA. Exhaust emissions and engine performance analysis of a marine diesel engine fueled with *Parinari polyandra* biodiesel–diesel blends. *Energy Rep*. 2020;6:2999-3007.
24. Badawy T, Mansour MS, Daabo AM, et al. Selection of second-generation crop for biodiesel extraction and testing its impact with nano additives on diesel engine performance and emissions. *Energy*. 2021;237:121605.
25. Dhahad HA, Fayad MA, Chaichan MT, Jaber AA, Megaritis T. Influence of fuel injection timing strategies on performance, combustion, emissions and particulate matter characteristics fueled with rapeseed methyl ester in modern diesel engine. *Fuel*. 2021;306:121589.
26. Duan X, Xu Z, Sun X, Deng B, Liu J. Effects of injection timing and EGR on combustion and emissions characteristics of the diesel engine fuelled with acetone–butanol–ethanol/diesel blend fuels. *Energy*. 2021;231:121069.
27. Subramani S, Govindasamy R, Rao GLN. Predictive correlations for NO_x and smoke emission of DI CI engine fuelled with diesel-biodiesel-higher alcohol blends-response surface methodology approach. *Fuel*. 2020;269:117304.
28. Sundar K, Udayakumar R. Comparative evaluation of the performance of rice bran and cotton seed biodiesel blends in VCR diesel engine. *Energy Rep*. 2020;6:795-801.
29. Perumal V, Ilangkumaran M. The influence of copper oxide nano particle added pongamia methyl ester biodiesel on the performance, combustion and emission of a diesel engine. *Fuel*. 2018;232:791-802.
30. Vara Lakshmi R, Jaikumar S, Srinivas V. A comprehensive review on the effect of nanoparticle dispersed diesel–biodiesel blends fuelled CI engine. *J Inst Eng India Ser C*. 2021;102:495-505.
31. Kanakraj S, Rehman A, Dixit S. CI engine performance characteristics and exhaust emissions with enzymatic degummed linseed methyl esters and their diesel blends. *Biofuels*. 2017;8(3):347-357.
32. Jena SP, Acharya SK, Das HC, Patnaik PP, Bajpai S. Investigation of the effect of FeCl₃ on combustion and emission of diesel engine with thermal barrier coating. *Sustain Environ Res*. 2018;28(2):72-78.
33. Yang WM, An H, Chou SK, et al. Emulsion fuel with novel nano-organic additives for diesel engine application. *Fuel*. 2013;104:726-731.

How to cite this article: Anbarasan B, Muralidharan K, Sakthi Rajan C, Rajkumar T. Cobalt chromite nanoparticle effects on kapok diesel emulsion performance and emission characteristics at various injection pressures. *Environ Prog Sustainable Energy*. 2024;e14385. doi:[10.1002/ep.14385](https://doi.org/10.1002/ep.14385)